Biophysical, photochemical and biochemical characterization of a protease from Aspergillus tamarii URM4634

da Silva, Osmar Soares; Silva, Jônatas de Carvalho; de Almeida, Elizane Melo; Sousa, Flávia; Gonçalves, Odete Sofia Lopes; Sarmento, Bruno; Neves-Petersen, Maria Teresa; Porto, Tatiana Souza

Published in:
International Journal of Biological Macromolecules

DOI (link to publication from Publisher):
10.1016/j.ijbiomac.2018.07.004

Publication date:
2018

Document Version
Accepted author manuscript, peer reviewed version

Biophysical, photochemical and biochemical characterization of a protease from Aspergillus tamarii URM4634

Osmar Soares da Silva, Jônatas de Carvalho Silva, Elizane Melo de Almeida, Flávia Sousa, Odete Sofia Lopes Gonçalves, Bruno Sarmento, Maria Teresa Neves-Petersen, Tatiana Souza Porto

PII: S0141-8130(18)31891-9
DOI: doi:10.1016/j.ijbiomac.2018.07.004
Reference: BIOMAC 10048

To appear in: *International Journal of Biological Macromolecules*

Received date: 20 April 2018
Revised date: 1 July 2018
Accepted date: 3 July 2018

Please cite this article as: Osmar Soares da Silva, Jônatas de Carvalho Silva, Elizane Melo de Almeida, Flávia Sousa, Odete Sofia Lopes Gonçalves, Bruno Sarmento, Maria Teresa Neves-Petersen, Tatiana Souza Porto , Biophysical, photochemical and biochemical characterization of a protease from Aspergillus tamarii URM4634. Biomac (2018), doi:10.1016/j.ijbiomac.2018.07.004

Biophysical, photochemical and biochemical characterization of a protease from *Aspergillus tamarii* URM4634

Osmar Soares da Silva[1#], Jônatas de Carvalho Silva[1#], Elizane Melo de Almeida[2], Flávia Sousa[3,4], Odete Sofia Lopes Gonçalves[5], Bruno Sarmento[3], Maria Teresa Neves-Petersen[5,6]; Tatiana Souza Porto*[1,2],

[1] - Northeast Biotechnology Network, Federal Rural University of Pernambuco, Rua Manuel de Medeiros, s/n - Dois Irmãos, Recife, Pernambuco, Brazil, 52171-900

[2] - Federal Rural University of Pernambuco, Academic Unity of Garanhuns, Avenida Bom Pastor, s/n - Boa Vista, Garanhuns, Pernambuco, Brazil, 55292-270.

[3] - i3S Instituto de Investigação e Inovação em Saúde, Universidade do Porto, Rua Alfredo Allen 208, 4200-135 Porto, Portugal; INEB – Instituto de Engenharia Biomédica, Universidade do Porto, Rua Alfredo Allen, 208, 4200-135 Porto, Portugal; CESPU, Instituto de Investigação e Formação Avançada em Ciências e Tecnologias da Saúde, Rua Central de Gandra 1317, 4585-116 Gandra, Portugal.

[4] - ICBAS – Instituto Ciências Biomédicas Abel Salazar, Universidade do Porto, Rua de Jorge Viterbo Ferreira 228, 4050-313 Porto, Portugal

[5] - Department of Health Science and Technology, Aalborg University, Frederik Bajers, 9220 Aalborg Ø, Denmark.

[6] - Department of Clinical Medicine, Aalborg University, Søndre Skovvej 15, 9000 Aalborg, Denmark.

# Contributed equally to the paper

*Corresponding author:

Tatiana Souza Porto

Tel.: +55 81 33206345.

E-mail address: portots@yahoo.com.br

Federal Rural University of Pernambuco, Academic Unity of Garanhuns.

Av Bom Pastor s/n, Boa vista 55290-000, Garanhuns, Pernambuco, Brazil.

ABSTRACT

Circular dichroism (CD) and fluorescence spectroscopy (FS) were used to monitor the pH-dependent conformational and structural stability changes induced by temperature and UV light on the protease from *Aspergillus tamarii* URM4634 at different pH values. The formation of photoproducts, such as N–formylkynurenine, dityrosine and kynurenine, were monitored with FS. The pH-dependent melting temperatures (T_m) were determined using CD and FS from 20 to 90°C. Conformational changes were correlated with the pH-dependent biochemical activities. CD revealed that the protease is rich in α-helices. Thermal denaturation was irreversible at all pH range and displayed T_m values from 42.8 to 67.8°C (CD) and from 38 to 60.3°C (FS), which the highest T_m was observed at pH 6. The light and temperature induced to the formation of photoproducts was more intense at high pH value. Despite the biochemical data shows optimum pH 9, the highest stability was at pH 6, maintaining 100% of activity after 24 h. The acquired data permits to select the best physicochemical parameters to secure the optimal activity and stability when used in biotechnological applications. Furthermore, the conformal changes induced by temperature in the protein are directly correlated with its level of biochemical activity.

Keywords: CD spectroscopy; Fluorescence spectroscopy; Protease.

1. INTRODUCTION

Aspergillus tamarii URM4634 is one strain of fungus isolated from Caatinga, a biome exclusive from Brazil [1], displayed the best performance concerning proteases production among thirty-four GRAS fungal strains [2]. Such a protease displayed collagenolytic and keratinolytic activities after purification, revealing the large applicability of this protease for industrial applications [3].

Due to their diverse origin, proteases can display different pH and temperature stability and activity profiles, different structures, molecular weight, isoelectric point, , conformational flexibility and glycosylation [4][5][6]. During the industrial process, the properties of a protein will be influenced by the local physical chemical environment that it is immersed in. Thus pH, salt, solvent, light and temperature are important factors that may affect the protein primary structure leading for some minor changes and destabilizing intramolecular interactions [7].

In particular, a change in pH value will change the charge distribution in the protein and the nature and extent of the electrostatic interactions [8][9]. Therefore, pH will modulate the thermostability of a protein and at extreme basic or acidic values, the protein may become significantly destabilized or even denature [10]. Moreover, the stability and stabilization of proteins structure is completed measuring their tolerance towards thermal stress [7]. Therefore, it is important to know the influence of these physicochemical parameters on the enzyme's structure and function. Such knowledge will provide insight into how to explore the biotechnological potential of such enzymes in different industrial processes.

Biophysical characterization of proteins provide information on the protein's structure under different physicochemical conditions essential to the understanding of their mechanism of action and regulation of biological activity [11].

In recent years, there has been an increasing use of fluorescence spectroscopy (FS) for protein characterization due to its low cost, rapid detection, high sensitivity, high efficacy, versatility, and high-throughput capability [12]. The intrinsic fluorescence of proteins can provide considerable information about protein structure and dynamics and is often used to study protein folding and molecular interactions. Tryptophan, which is the intrinsic fluorophore with the largest extinction coefficient and the largest quantum yield, is generally present at about 1.3 % in proteins [13]. Trp is an excellent intrinsic probe used to monitor protein conformational changes since its range of spectral fluorescence emission is solvent sensitive. Moreover, when exposed an external quencher probe, tryptophanyl fluorescence is very solvent sensitive [14].

When in an apolar environment its fluorescence is blue shifted compared to when being in a polar environment, where it emits at longest wavelengths [15]. Light is another factor that induces protein conformational changes. UV excitation of the protein's aromatic pool, i.e., tryptophan (Trp), tyrosine (Tyr) and phenylalanine (Phe), also leads to protein conformational changes [16]. UV light induced photo-oxidation of, i.e., tryptophan and tyrosine residues lead to photochemical products, such as, kynurenine, N–formylkynurenine and dityrosine and to the disruption of disulfide bridges in proteins. The formation of such photoproducts can also be monitored with fluorescence spectroscopy since such products have different spectral properties [17].

Circular dichroism (CD) is another biophysical technique that is vastly used in order to monitor protein conformational changes induced by, i.e., pH, light and temperature. CD provides not only information about the secondary structural content

of the protein (far-UV CD) but also information about the tertiary structure of the protein (near-UV CD) [11].

Fluorescence spectroscopy together with circular dichroism (CD) in the far-UV range (used to monitor changes in the secondary structure of a protein) allows for a more complete biophysical characterization of the protein [18]. The present study aimed at understanding the effect of pH, UV light and temperature on the structure, formation of photoproductcs and in the denaturation process of the novel protease from *Aspergillus tamarii* URM4634. The thermal stability of this new enzyme was monitored as a function of pH using circular dichroism and fluorescence spectroscopy and correlated with his pH-activity and stability profile.

2. MATERIALS AND METHODS

2.1. Microorganism maintenance and Inoculum preparation

Aspergillus tamarii URM4634 strain was kindly supplied from the URM culture collection from Federal University of Pernambuco, Brazil. It was preserved in mineral oil and maintained at 28°C in Czapek Dox Agar. The inoculum spores were obtained by grow up in inclined Czapek Dox Agar tubes for 7 days at 30ºC. The spores were collected with addition of 3 mL of NaCl (0.9%) and Tween 80 (0.01%) sterilized solution.

2.2. Protease production

Solid-state fermentations (SSF) were carried out for 72 h at 30°C in 125 mL Erlenmeyer flasks containing 5 g of wheat bran flour and inoculum 10^7 spores/mL calculated to correspond 40% of initial moisture. The proteolytic extract was recovered by addition of 7.5 mL of 0.1 M sodium phosphate solution (pH 7.0) per gram of fermented material and homogenized in shaker for 2 h. Solids were finally removed from the filtrate by centrifugation at 3000 ×*g* (Thermo Fisher ScientificST16R, Germany) for 15 min at 4 °C, and the supernatant was used as crude extract.

2.3. Purification by ion-exchange chromatography

To test its adsorptive character, an aliquot of 100 mL of crude extract was precipitated with acetone 70% and centrifuged at 3000 ×*g* and 4°C for 20 min. After discarding the supernatant, the pellet was re-suspended with 20 mM Tris-HCl (pH 8.0) and submitted to the next purification step using ion-exchange chromatography. The adsorptive character of the pre-purified extract was loaded on a 1.5 × 30 cm column packed with DEAE-sephadex A50 pre-equilibrated with 20 mM Tris-HCl (pH 8.0). Proteins were eluted with a linear gradient of NaCl (0-0.7M) with 20 mM Tris-HCl (pH 8.0) at a flow rate of 60 mL/h and detected using a UV/VIS spectrophotometric detector at λ 280 nm.

2.4. Analytical determinations

Proteolytic activity was determined by the method of Ginther [19] modified as follows. Azocasein (Azo dye-impregnated casein) was dissolved in 50 mL of 0.2 M phosphate buffer (pH 7.2) containing 1.0 mM $CaCl_2$ up to a concentration of 1% (w/v).

After incubation of 0.15 mL of enzyme extract and 0.25 mL of azocasein solution for 1 h at 25°C, the reaction was stopped by adding 1.0 mL of 10% (w/v) trichloroacetic acid. Samples were centrifuged at 8000 ×*g* (Hettich-Zentrifugen MIKRO 200 R, Germany) for 20 min at 4°C, and 0.8 mL of the supernatant were added to 0.2 mL of 1.8 M NaOH. A proteolytic enzyme unit was defined as the amount of enzyme able to lead to a 0.1 increase in absorbance at 420 nm within 1 h. The total protein concentration was determined according to Bradford [20] using Coomassie Brilliant Blue G-250 as dye and Bovine Serum Albumin as the standard protein. The specific activity was calculated as the ratio of proteolytic activity (U/mL) to total protein concentration in the sample (mg/mL) and expressed in U/mg.

2.5 Steady-state fluorescence spectroscopy studies

Protease solutions (5 μM) were prepared in different 0.05 M buffers: acetate buffer pH 5; phosphate buffer pH 6, 7.2 (same pH of the activity), 8; glycine buffer (pH 9, 10 and 11).

2.5.1. Acquisition of steady-state fluorescence spectra

Steady-state fluorescence emission intensity spectra were collected upon 280 nm excitation of tryptophan and tyrosine residues (emission from 300-530 nm), and upon 295 nm excitation (emission from 315–530 nm) to selectively excite tryptophan residues. Excitation spectra were also acquired from 200-300 nm with emission fixed at 345 nm. All measurements were conducted on a Felix fluorescence RTC 2000 spectrometer (Photon Technology International, Canada, Inc.347 Consortium Court

London, Ontario N6E 2S8) with a T-configuration, using a 75-W Xenon arc lamp coupled to a monochromator. The samples were analyzed in a quartz cuvette high precision with a 10 mm x 2 mm light path. The excitation and emission slit widths were set to 0.25 and 6.0 mm, respectively. The excitation power was 2.5 μW at the entrance of the excitation chamber. Fluorescence excitation and emission spectra were analyzed before thermal unfolding at 20°C, upon reaching 90°C and after cooling the sample to 20°C as a function of pH. During the heating process from 20 to 90°C and cooling down from 90 to 20°C, the sample was illuminated with 280 nm light with a heating and cooling rate of 1°C/min, totalizing 140 min of continuous illumination. Changes in fluorescence excitation and emission intensity were quantified. Normalized emission and excitation spectra were obtained by dividing each data point by the maximum intensity value in each spectrum in order to calculate putative blue and red shifts induced by pH and temperature.

Fitting procedures were done using Origin 8.1 (OriginLab Corporation, Northampton, MA, USA). Emission and excitation spectra were first smoothed using 10 points adjacent averaging and all Raman corrected by subtracting the spectra recorded for the buffer in solution at each respective pH value.

2.5.2. Thermal unfolding studies and melting point determination using fluorescence spectroscopy

The experimental denaturation and renaturation studies were conducted in order to determine the melting point (T_m) of the protein as a function of pH value. The fluorescence emission intensity at 345 nm of fresh protease sample upon 280 nm excitation was monitored from 20 to 90°C at every pH value. The heating rate was fixed

at 1°C/min. During the heating process, the sample was illuminated with 280 nm light, with a power of 2.5 μW, totalizing 70 min of illumination. The first derivative of each 5 points smoothed datasets was acquired in Origin version 8.1 (OriginLab Corporation, Northampton, MA, USA) in order to calculate the melting temperature of the protein as a function of pH value. The decay curves were fitted by the Boltzmann function using the following decay model:

$$y = A2 + \frac{A1-A2}{1+ e^{(X-Xo)/dX}} \quad (1)$$

where A_1 and A_2 are the fit parameters corresponding to initial and final fluorescence intensity, X_0 the central point and dX the time constant.

2.5.3. Photoproducts of tryptophan and tyrosine residues

Fluorescence excitation and emission spectra from Trp and Tyr photoproducts (N–formylkynurenine, dityrosine and kynurenine) were monitored before (at 20°C) and after (at 90°C and when cooled to 20°C) thermal unfolding. During the heating process from 20 to 90°C and during the cooling down step from 90 to 20°C, the sample was illuminated with continuous 280 nm excitation (lamp power of 2.5 μW, measured at the entrance of the excitation chamber). A heating and cooling rate of 1°C/min was used, totalizing 140 min of 280 nm excitation. All measurements were conducted on a Felix fluorescence RTC 2000 spectrometer (Photon Technology International, Canada, Inc. 347 Consortium Court London, Ontario N6E 2S8) with a T-configuration, using a 75-W Xenon arc lamp coupled to a monochromator. The samples were analyzed in a quartz cuvette high precision with a 10 mm x 2 mm light path. The excitation and emission slit

widths were set to 0.25 and 6.0 mm, respectively. The fluorescence excitation and emission spectra of such photoproducts differ from the fluorescence spectra of Trp and Tyr according to the literature. N–formylkynurenine displays absorption peaks at 261 and 322 nm and its emission peaks between 400 to 440 nm. The ionized and non-ionized forms of dityrosine have absorption maxima at 315 nm and 283 nm, respectively and they maximally emit in a range between 400-409 nm. Kynurenine displays absorption peaks at 258 and 360 nm and shows fluorescence emission maxima between 434 and 480 nm [21][22][23]. Therefore, their formation can be monitored using fluorescence spectroscopy. Fluorescence emission spectra of fresh and of illuminated samples were acquired upon 320 nm excitation (emission from 360-530 nm) and upon 360 nm excitation (emission from 419-530 nm). Fluorescence excitation spectra were acquired with emission set to 405 and 435 nm.

2.6. Circular dichroism spectroscopy

The secondary structure of the protease from *Aspergillus tamarii* URM4634 at different pH and different temperature values was monitored by CD spectroscopy. Far-UV CD spectra were obtained with a Jasco J815 CD Spectrophotometer (Jasco Incorporated, Easton, U.S.A.) and the lamp housing was purged with nitrogen. The spectra were monitored from 200 to 260 nm using a bandwidth of 1 mm, a data integration time of 4 s, a data pitch of 0.5 nm, and a scanning speed of 50 nm/min. The concentration of the protease was adjusted to 100 μg/mL by diluting the stock solution in different buffers. 0.4 mL of the sample was used in 0.1 cm cell. All spectra were the average of 8 scans, leading to 10 min of acquisition time for each sample. The CD spectrum of the buffer was subtracted from the sample spectrum and smoothed using 10

points smoothing. The spectra at 20°C, after heating at 90°C and after cooling at 20°C were obtained and compared, at each pH value.

2.7. Thermal unfolding studies and melting point by circular dichroism

Thermal denaturation of the protease was measured by monitoring the intensity of ellipticity at different pH values over the temperature range from 20 to 90°C. During heating, a heating rate of 1°C/min was used, totalizing 70 min of illumination. All samples were placed in a 1 mm path length cuvette. The experimental denaturation profiles were smoothed, using 10 points smoothing routine, fitted and normalized using the Origin 8 software (OriginLab Corporation, Northampton, MA, USA) to calculate the melting temperature (T_m). The decay curves were fitted by the Boltzmann function according to equation 1.

2.8. Effect of pH on proteolytic activity and stability

The effect of pH on the enzyme's stability was carried out by previously incubating the purified enzyme in different 0.2 M buffers at 5°C: Acetate (pH 5.0 – 6.0), phosphate-phosphate (pH 7.2 – 8.0) and glycine-NaOH (pH 9.0 -11.0). Afterwards, the protease activity of each of these protein solutions was monitored at time intervals 0 h and 24 h, at pH optimum 7.2, as described in section 2.4.

Furthermore, the pH-activity profile of the enzyme was also monitored as described in section 2.4 with the following change: the protease was incubated with the azocasein solution 1% prepared in different buffers at different pH values using acetate

(pH 5.0 – 6.0), phosphate-phosphate (pH 7.2 – 8.0) and glycine-NaOH (pH 9.0 -11.0) buffers.

3. RESULTS AND DISCUSSION

3.1 Secondary structure analysis monitored by circular dischroism spectroscopy

In previous studies reported by Silva et al. [3], the protease from *Aspergillus tamarii* URM4635, which was totally purified by ion exchange DEAE-sephadex A50 chromatography, displayed molecular weight of 49.3 kDa, purification factor of 6.9 and yielded 62.0% of its initial activity. This protease also showed collagenolytic and keratinolytic activity. Collagenases have several therapeutic properties in wound healing, burns, nipple pain and some diseases including intervertebral disc herniation, keloid, cellulite, lipoma among others [24]. Keratinases are widely used in various application fields, such as leather, textile, feed, fertilizers and cosmetics industries [25]. These reveal the large applicability of the protease from *Aspergillus tamarii* URM4634. The biophysical and biochemical characterization of enzymes provides important data useful to industrial applications. Enzymes that maintain the activity for long periods of time and that present high activity over a broad range of pH or temperature values are relevant to industry. However, during the process such agents might led to denaturation of the protein. In addition, some enzymes can present a range of temperatures where reversible denaturation is observed, but outside that range, denaturation is irreversible [26]. The use of biophysical techniques allows for a fast and reliable quantification of the protein's stability as a function of, e.g., temperature and pH. Such data can be correlated with the respective protein temperature and pH profiles. In the present paper,

conformational changes in the secondary structure of the protease induced by different pH and temperature values were detected by circular dichroism and fluorescence spectroscopy. The sample was heated from 20 to 90°C at different pH values and cooled back to 20°C in order to understand the denaturation and putative refolding process.

CD data revealed pH and temperature induced conformational changes in the secondary structure of the protein. In Fig. 1A are displayed the spectra of the fresh protease at 20°C and at different pH values. At all pH values, the spectra displayed two minima at 209±1 nm and 220±2 nm and positive inflection around 195 nm, which is a typical feature for a protein rich in α-helices [27][28]. This is explained by the protein with secondary structure α-helice presenting an asymmetry conformation. The asymmetry is due of the turns that the amino acids. The spectrum at pH 9 presented the largest ellipticity intensity (negative intensity values) while the lowest values were observed at pH 11 (Fig. 1A). A blue shift has occurred in the CD signal at pH 11 relative to pH 9 the ellipticity peaks shifted from 210 and 221 nm to 208 and 218 nm (negative intensity values) but, still characteristic of α-helices.

After heating the samples until 90°C (Fig. 1B), the spectra of the protease did not maintain the spectral characteristic of α-helices. The protease revealed thermal denaturation at all pH values showing a peak around 204±2 nm. This indicates that the secondary structure of protease has changed from being rich in α-helices into random coil peak between 203-206 nm [29].

After cooling the sample back to 20°C, it was not possible to see refolding of the structure at all pH values except at pH 9, where the characteristic two ellipticity peaks associated to α-helical structure were observed. However, the peaks have suffered a blue shift from 210 and 221 nm (fresh sample at 20°C) to 204 and 219 nm (Fig. 1C). No clear peaks have been observed at pH 5 and 6 after cooling (Fig. 1C). CD data showed

that at pH 7.2, 8, 10 and 11 the temperature induced a loss of secondary structure since the cooled spectra displayed a single peak around 205±1 nm (Fig. 1C).

Another study also was carried out to monitor the conformational changes induced by temperature increase. The CD spectra of the protease were acquired at different temperatures from 20 to 90°C, at 10°C intervals, at pH 9 (Fig. 1D). It was observed that from 20 to 40°C, the protease was very stable and displayed two maximum negative peaks at 210 and 221 nm. At 50°C, the ellipticity intensity decreased and suffered a red-shift (210 and 223 nm), comparing to spectrum of the sample at 20°C. After 60°C the loss of secondary structure was evident with a continuous decrease in the intensity of ellipticity and the protein became a random coil showing peaks between 205-210 nm.

3.2 Conformational analysis using fluorescence spectroscopy

The conformational changes induced by pH and temperature on the protease were investigated by fluorescence spectroscopy. The sample was excited at 280 nm in order to monitor the fluorescence emission spectrum of the protease. The emission was set to 345 nm when acquiring the excitation spectrum, since this is the wavelength corresponding to maximum fluorescence emission intensity of the protease from *Aspergillus tamarii* URM4634 when excited at 280 nm in phosphate buffer at pH 9. This pH was chosen as a reference since this is the pH where maximum proteolytic activity was observed (see Fig. 9B).

In order to detect conformational changes induced by temperature, the fluorescence spectra were acquired at 20°C (Figs. 2A and B), upon heating at 90°C and upon cooling to 20°C (Figs. 2C and D) for all pH values. The fluorescence excitation

and emission intensities increased from acidic to alkaline pH (Figs. 2A and E). At the studied pH values, the wavelength corresponding to the fluorescence emission maximum (λ_{max}) varied between 338 and 352 nm (Figs 2B and 2F, fresh sample at 20°C) and the observed trend was that the more alkaline the pH, the more red shifted λ_{max} was (except from pH 5 to pH 6, where a 3 nm blue shift has been observed). The same behavior was observed during the biochemical characterization since it was observed that the activity decreased from pH 5 to 6 but increased from pH 6 to its optimum pH 9.0 (Fig. 9B, pH-activity profile).

The fluorescence spectral properties of tryptophan are known to be modulated by solvent polarity and by the presence of fluorescence quenchers. Trp fluorescence emission is known to be very sensitive to the dielectric constant and therefore to the polarity of the medium surrounding it. In polar environments, the fluorescence emission is red shifted compared to the Trp's emission in apolar environments [17]. Indeed, the dielectric constant is correlated with the polarization of the material [30]. Proteins have a specific interaction within a solvent environment that affects their dielectric relaxation mechanisms [31]. In polar environments there is a reorganization of the solvent's polar molecules along the electric field lines generated by dipoles in the protein [32] and as a consequence, the system relaxes and the protein will emit at longest wavelengths [16].

When the sample was heated up to 90°C, a loss of the fluorescence intensity was observed at all pH values. The loss was less strong at pH 8 and most evident at pH 11 (Table 1). At high temperature, the solvent molecules populate high vibrational state and such vibration causes more frequent collisions between the solvent molecules and protein, leading to quenching. Different photochemical pathways will lead to an increase or to a decrease of the protein's fluorescence emission intensity. An increase can be caused by light induced disruption of SS bridges, known to be one of the best

quenchers of protein fluorescence [33]. A decrease of fluorescence emission intensity may be due to either the photodestruction of the native fluorophores or due to an increase of fluorescence quenching as the result of closer distances to quencher groups as a result of protein conformational changes [34].

After heating the sample up to 90°C and cooling it back to 20°C (Figs. 2C, 2D and 2E) a similar trend was observed: the more alkaline the pH, the more red shifted λ_{max} was, peaking between 345 and 355 nm (Fig 2D). Additionally, the spectral blue shifts observed after warming up the sample to 90°C at pH values from 9 to 11 and the spectral red shifts observed after cooling down the samples to 20 °C to all pH values are displayed in Figure 2F. It indicated that temperature induced conformational changes in the structure leaving the Trp residues more solvent exposed.

Fig. 3 shows one example of the protease spectra before heating, upon heating and upon cooling obtained at pH 6. It can be observed that the fluorescence excitation and emission intensity decreased by -81.7% and -80.7%, respectively, upon heating the sample up to 90°C. Although the fluorescence excitation and emission intensities increased when the sample was cooled down to 20°C, the signal did not completely recover the initial emission (-22.1%) and excitation (-28.4%) intensity (Table 1). When the sample was cooled down to 20°C, its fluorescence emission spectrum suffered a red shifted from 338 nm (fresh sample) to 346 nm (Figs 2F and 3).

In order to selectively monitor the fluorescence emission spectra for the tryptophan moiety in the studied protease, the protein was excited at 295 nm. Emission spectra were acquired at 20°C (Figs. 4A and B, fresh sample), upon heating the sample up to 90°C and upon cooling it down at 20°C (Figs. 4C and D), at pH 5, 6, 7.2, 8, 9, 10 and 11. At 20°C before heating, the wavelengths corresponding to the maximum fluorescence emission intensity at the different pH values were observed from 335 to

353 nm (Fig. 4B, E and F, fresh sample at 20°C). Tyr emits like Tryptophan when its phenolic OH group is ionized. Such ionization is expected because the Tyr side chain pKa is around 10.5 in the ground state. Tyrosinate emission can be most easily observed at high pH, where the phenolic OH group is ionized in the ground state. Interestingly, such pKa falls to about 4 in the excited state and therefore, ionization can even occur at neutral pH. The fluorescence emission intensity can be quenched because a weakly basic group can remove the phenolic proton [35], as example, the pH 5 (Fig. 2A and 4A), prepared using acetate buffer, which has a weakly basic group, showed the lowest fluorescence intensity. Furthermore, fluorescence emission intensity decreases in the presence of fluorescence quenchers. These quenchers can be an amide-aromatic hydrogen bond or adjacent disulfide bridge [36]. Protonated side chains and thiol groups are also known to quench protein fluorescence.

After heating up the sample to 90°C, a red-shift of λ_{max} (when compared to the λ_{max} of the fresh sample at 20°C) is observed at pH values from 5 to 8, and a blue-shift is observed from 9 to 11 (Fig. 4F). This behavior corroborates with the data found upon excitation at 280 nm, except at pH 5 where no shift was observed (Fig. 2F). After cooling down the sample to 20ºC, the fluorescence emission suffered a red-shift from 335-353 nm to 344-358 nm (Fig. 4C and D) and a loss in the fluorescence emission intensity is observed when compared to the fresh sample (Fig. 4E).

Table 1 shows the wavelength at which the maximum excitation and emission intensities (λ_{max}) have been observed for the fresh sample at 20ºC, as a function of pH value. The excitation spectra of the fresh sample at 20ºC obtained fixing emission at 345 nm showed that λ_{max} occurred at 286± 1nm. Furthermore, it also displays the intensity changes in the fluorescence emission and excitation spectra (upon excitation at 280 and 295 nm and upon fixing the emission at 345 nm, respectively) at the respective

λ_{max}, as a function of pH and temperature. The largest drop in the fluorescence emission intensity monitored after cooling is observed at pH 5 and 6. After cooling down, the largest fluorescence emission intensity (upon excitation at 295 nm) decay was observed to be -34.3% at pH 6 and the smallest decay of 10.8% was observed at pH 10. Furthermore, the fluorescence emission intensity data (exc. 280 nm) of the cooled samples at 20°C shows that the protease at pH 5 lost 26.5% of the initial fluorescence emission intensity, the largest loss observed, and 7.2% at pH 10, the smallest observed loss (Figure 2E and Table 1). When analyzing the fluorescence excitation spectra obtained with emission fixed at 345 nm, at the different temperatures, it can be observed that at 90°C the fluorescence signal lost around 77.9 to 88.0% of the initial excitation intensity at all pH value, but when cooled to 20°C the protease lost from 26.5% (pH 5) to 13.5% (pH 11) of the initial fluorescence excitation intensity. As showed in Figs. 2F and 4F, the λ_{max} suffered a red shift from 338-352 nm to 345-355 nm at all pH values upon cooling the protein sample relative to the λ_{max} observed for the fresh sample. Fig. 5 displays the changes induced by temperature in the wavelength at which maximum protein fluorescence emission intensity is observed ($\Delta\lambda=\lambda_{(20°C\ before\ eating)} - \lambda_{(20°C\ after\ cooling)}$). During the heating run the protein has been excited at 280 or at 295 nm. Data has been retrieved from panels F in Figures 2 and 4. When analyzing the $\Delta\Delta\lambda$ (defined as $\Delta\lambda_{(exc.\ 280nm)} - \Delta\lambda_{(exc.\ 295nm)}$) at pH 6 and 7.2, it can be observed that the sample suffered an additional shift of 3 nm when excited at 295 nm compared to 280 nm.

3.3. Formation and detection of Photoproducts

The peptide backbone, Trp, Tyr, Phe, and cystine residues are the primary targets of photodegradation in proteins [37]. UVB excitation of aromatic residues in proteins leads to the disruption of SS bridges and to the formation of photoproducts [38], such as N-formylkynurenine (NFK), kynurenine (Kyn), dityrosine (DT), isodityrosine, trityrosine and pulcherosine [39]. Light at 320 nm excites both NFK, Kyn and DT, and at 360 nm excites NFK and Kyn but does not excite DT [16].

In order to detect the pH-dependent formation of photoproducts, fluorescence emission spectra of the protein were acquired upon excitation at 320 nm and the excitation spectra of the protein were acquired upon fixing the emission at 405 nm (Fig. 6). Additional fluorescence emission spectra have been acquired upon excitation at 360 nm and additional excitation spectra have been acquired fixing the emission at 435 nm (Fig. 7). All spectra were acquired at 20°C, before heating the sample from 20 to 90°C and after cooling the sample from 90 to 20°C. Figs. 6A and 7A display the spectra for the fresh sample at 20°C and the presence of photochemical products can be observed, peaking the fluorescence emission intensity between 400 and 430 nm, upon excitation at 320 nm (Fig. 6A) clearly visible at pH 5, excluding the initial data around 360 to 380 nm and between 435 and 446 nm, with excitation fixed at 360 nm. The peaks upon excitation at 320 nm are characteristics of NFK, which fluorescence peaks between 400 to 440 nm and of DT emission, known to peak from 400 to 409 nm [17][27][40]. Kyn is also excited at 320 nm but it emits in range between 434 to 480 nm.

At pH 5, the sample displayed the lowest fluorescence emission intensity, and it increased from acidic to alkaline pH values between 17.4-32.8% and 8.2-29.7%, upon excitation at 320 and 360 nm, respectively (Fig. 6A and 7A). The intensity of such spectra has increased after heating the sample to 90°C and cooling it down to 20°C from 9.1% (pH 5) to 59.7% (pH 11), and from 9.1% (pH 5) to 90.8% (pH 11) upon excitation

at 320 and 360 nm, respectively (Fig. 6B and 7B). The intensity of excitation intensity spectra increased accordingly, having been observed an increase from 14.7% (pH 5) to 69.4% (pH 11) when emission is fixed at 405 nm (Figs. 6C and 6D) and from 9.9% (pH 5) to 79.6% (pH 11) when emission is fixed at 435 nm (Figs. 7C and 7D).

Photoexcitation of the aromatic residues of proteins is known to lead to the ejection of electrons from their aromatic side chains. Such electrons will be caged by water molecules, leading to the formation of solvated electrons, e_{aq}^-, a transient species that will lead to the formation of photoproducts. High pH values are known to favor the formation of solvated electrons with longer transient lifetime, while low pH leads to lower concentrations of solvated electrons with shorter transient lifetime [37]. The solvated electron can react with a nearby disulfide bridge (RSSR) forming a disulfide electron adduct ($RSSR^{\bullet -}$) [37]. On other hand, photoionization of Trp residues may form an excited tryptophan that can undergo intersystem crossing, yielding a triplet state ^{3}Trp, which may also lead to the disruption of a nearby disulfide bridge. Tyrosine residues may also undergo non-radiative decay, fluorescence decay, or undergo intersystem crossing to the triplet state (^{3}Tyr-OH). It can also be photoionized, at neutral pH, by absorbing a second photon from the triplet state leading to the formation of a solvated electron and radical cation adduct ($Tyr\text{-}OH^{\bullet +}$). This will give rise to a neutral radical ($Tyr\text{-}OH^{\bullet}$) that results from the rapid deprotonation of the radical cation. At high pH followed by photoionization, the radical $Tyr\text{-}OH^{\bullet}$ can lead to formation of the neutral radical ($Tyr\text{-}O^{\bullet}$) also giving rise to a solvated electron and disulfide electron adduct ($RSSR^{\bullet -}$). A nearby Trp or disulfide bridge rapidly quenches the triplet state of Tyr. The disulfide electron adduct easily dissociates leading to a broken disulfide bridge ($RS^{\bullet}$ + RSH) and formation of photoproducts [37][36].

3.4 Correlation between fluorescence and circular dichroism spectroscopy thermal scannings

Protein stability, particularly the resistance to high temperatures, is a key parameter for all processes involving enzymes [18]. To determine the melting temperature of the protein of *Aspergillus tamarii* URM4634 at different pH values, studies were carried out in fluorescence and circular dichroism spectroscopy.

Fig. 8 shows the pH-dependent denaturation curves of the protease obtained by CD (Fig 8A) and fluorescence spectroscopy (Fig 8B). As described at section 2.7, the denaturation curves acquired by CD were smoothed (10 points), fitted (Boltzmann function) and normalized. The denaturation curves obtained by fluorescence spectroscopy were smoothed with 5 points (Fig 8B) and fitted using the Boltzmann function. Fig. 8C presents one example of a fitted and normalized decay curve, at pH 5, and the first derivative of the fitted Boltzmann function. The derivative procedure reveals the minimum point of the curve, equivalent to the melting point (T_m). All denaturation curves were obtained increasing the temperature from 20 to 90°C.

The enzyme was cooled down from 90 to 20°C, at a cooling rate of 1°C/min and both fluorescence emission and CD ellipticity intensity were monitored during such process to monitor a possible refolding of the protein. However, no transitions were found (Fig, 8D, CD data not shown).

All fitted parameter values with the corresponding errors, T_m, adjusted R square are displayed in Table 2. The pH dependent transition temperatures recovered with fluorescence spectroscopy were found between 37.8 and 60°C, and the ones recovered with CD were observed from 42.8 to 67.8°C. From pH 5 to 7.2, data obtained with fluorescence spectroscopy revealed a minor variation of the respective T_m values (up to

≈ 1°C). However, CD data showed to be more sensitive to pH changes, being observed a maximum T_m variation of ≈ 10.4°C at those pH values. CD data showed that the protease presents its largest thermal stability value at pH 6.0 (67.8°C). The normalized and fitted denaturation curve obtained by CD spectroscopy at pH 6 (Fig. 8A) also showed a different behavior corresponding to a larger T_m.

As shown in Fig. 9A, the T_m's determined by fluorescence spectroscopy were lower than the values obtained with CD spectroscopy, except at pH 7.2 where the T_m obtained by fluorescence spectroscopy was maximally 1.8°C higher than the value obtained by CD. According to Sousa et al. (2017) [41] the different T_m values recovered derived from the basic difference in both spectroscopies: fluorescence spectroscopy will give us information about conformational changes induced by temperature and felt by the aromatic amino pool of the protein, where CD spectroscopy reports global secondary structural changes in the whole protein.

In order to correlate the thermal stability data obtained by fluorescence and CD spectroscopy with the biological activity, biochemical characterization of the protease was carried out using the same buffer solution used while carrying out fluorescence and CD spectroscopy. Fig. 9B is shows that the protease showed its highest stability at pH 6, maintaining 100% of its initial activity after 24 h of incubation at 5°C. The biophysical data is positively correlated with biochemical data, both showing the highest stability of the protease of *A. tamarii* URM4634 at pH 6 in acetate buffer. Previous data showed that the highest stability of the protease from *A. tamarii* URM4634 was observed at pH 7 (data not shown), although such characterization was carried out using citrate buffer at pH values from 5 to 7. It means that the stability and activity not depend only on the pH value but also on the buffer used. Despite the optimum pH 9, which showed positively correlation with the most intense CD signal, it did not present the highest stability (Fig.

9B). An increase in thermostability is often accompanied by a decrease in activity and vice versa, even though this cannot be considered a general rule. An optimum compromise between these opposite tendencies should then be looked for so as to select the best conditions under which to perform an industrial process [42].

The irreversible thermal denaturation of a protein, according to Carvalho *et al.* [18], can be described by the classical scheme as ($N_{(k1)} \leftrightarrow_{(k2)} U \rightarrow_{(k3)} D$) where N is the native state, U is the reversible denatured state, and D is a final irreversible state. This model can be converted into a single step model (N→D) assuming that k_1, k_2, and k_3 are all first order kinetic constants and $k_3 >> k_2$. In this case, no equilibrium between N and U is established during denaturation. Therefore, all U molecules formed are preferentially converted into D instead of refolding to form N. The concentration of U molecules is negligible in this case and the denaturation depends only on k1. After heating to 90°C, the protease was cooled back to 20°C aiming to verify if the structure refolded. The results showed that the thermal denaturation of the protease was irreversible at all pH values.

4. CONCLUSIONS

The present work showed the relationship between pH induced protein conformational changes and changes in its biological pH dependent activity. The spectroscopy techniques were useful in monitoring structural changes as a function of pH, temperature and UV light. The protease from *Aspergillus tamarii* URM4634 showed the highest stability at pH 6, however the thermal denaturation observed at all pH values was irreversible. Data from CD spectroscopy were cleaner than fluorescence spectroscopy to determine the T_m values. After cooling, the formation of photoproducts

was observed at all pH values, especially in the alkaline pH range. The protease from *Aspergillus tamarii* URM4634 has great applicability in industrial process. Therefore, the presented biophysical and biochemical data is relevant to apply this enzyme in biotechnological applications.

5. ACKNOWLEDGEMENTS

Osmar Soares da Silva is grateful to FACEPE (*Foundation for Science and Technology of the State of Pernambuco*, Recife, Brazil) for the PhD scholarship (process IBPG-0257-5.07/14). Jonatas Silva would like to thank CAPES (*National Council for the Improvement of Higher Education*, Brasília, Brazil) by the exchange scholarship CSF-PVE-S- 88887.122755/2016-00 and FACEPE by the PhD scholarship IBPG-0514-5,07/14. Flávia Sousa would like to thank to FCT for funding the PhD scholarship (SFRH/BD/112201/2015. This article is a result of the project NORTE-01-0145-FEDER-000012, supported by Norte Portugal Regional Operational Programme (NORTE 2020), under the PORTUGAL 2020 Partnership Agreement, through the European Regional Development Fund (ERDF). This work was also financed by FEDER - Fundo Europeu de Desenvolvimento Regional funds through the COMPETE 2020 - Operacional Programme for Competitiveness and Internationalisation (POCI), Portugal 2020, and by Portuguese funds through FCT - Fundação para a Ciência e a Tecnologia/ Ministério da Ciência, Tecnologia e Ensino Superior in the framework of the project "Institute for Research and Innovation in Health Sciences" (POCI-01-0145-FEDER-007274).

6. REFERENCES

[1] K. Ribeiro, E.R. Sousa-Neto, J.A. Carvalho, J.R.S. Lima, R.S.C. Menezes, P.J. Duarte-Neto, G.S. Guerra, J.P.H.B. Ometto, Land cover changes and greenhouse gas emissions in two different soil covers in the Brazilian Caatinga, Sci. Total Environ. 571 (2016) 1048–1057.

[2] O.S. Silva, R.L. Oliveira, C.M. Souza-Motta, A.L.F. Porto, T.S. Porto, Novel Protease from *Aspergillus tamarii* URM4634: Production and characterization using inexpensive agroindustrial substrates by solid-state fermentation, Adv. Enzym. Res. 04 (2016) 125–143.

[3] O.S. da Silva, E.M. de Almeida, A.H.F. de Melo, T.S. Porto, Purification and characterization of a novel extracellular serine-protease with collagenolytic activity from *Aspergillus tamarii* URM4634, Int. J. Biol. Macromol. 117 (2018) 1081–1088.

[4] T.P. Nascimento, A.E. Sales, T.S. Porto, R.M.P.B. Costa, L. Breydo, V.N. Uversky, A.L.F. Porto, A. Converti, Purification, biochemical, and structural characterization of a novel fibrinolytic enzyme from *Mucor subtilissimus* UCP 1262, Bioprocess Biosyst. Eng. 40 (2017) 1209–1219.

[5] R.S. Jayani, S. Saxena, R. Gupta, Microbial pectinolytic enzymes: A review, Process Biochem. 40 (2005) 2931–2944.

[6] R.H. Khan, S. Rasheedi, S.K. Haq, Effect of pH, temperature and alcohols on the stability of glycosylated and deglycosylated stem bromelain, J. Biosci. 28 (2003) 709–714.

[7] S.K. Haq, R.H. Khan, Spectroscopic analysis of thermal denaturation of *Cajanus cajan* proteinase inhibitor at neutral and acidic pH by circular dichroism, Int. J.

Biol. Macromol. 35 (2005) 111–116.

[8] M.T. Neves-Petersen, S.B. Petersen, Protein electrostatics: A review of the equations and methods used to model electrostatic equations in biomolecules - Applications in biotechnology, Biotechnol. Annu. Rev. 9 (2003) 315–395.

[9] M.T. Neves-Petersen, E.I. Petersen, P. Fojan, M. Noronha, R.G. Madsen, S.B. Petersen, Engineering the pH-optimum of a triglyceride lipase: From predictions based on electrostatic computations to experimental results, J. Biotechnol. 87 (2001) 225–254.

[10] S.B. Petersen, P. Fojan, E.I. Petersen, T.M. Neves-Petersen, The Thermal Stability of the *Fusarium solani pisi* Cutinase as a Function of pH, J. Biomed. Biotechnol. 1 (2001) 62–69.

[11] S.M. Kelly, T.J. Jess, N.C. Price, How to study proteins by circular dichroism, Biochim. Biophys. Acta. 1751 (2005) 119–139.

[12] H.R. Qomi, A. Habibi, S.M. Shahcheragh, Spectrochimica Acta Part A : Molecular and Biomolecular Spectroscopy Synthesis and fl uorescence studies of nine 1,5-benzodiazepine-2,4-dione derivatives : Dual emission and excimer fluorescence, Spectrochim. Acta Part A Mol. Biomol. Spectrosc. 174 (2017) 164–170.

[13] T.E. Creighton, PROTEINS: Structures and Molecular Properties, 1993.

[14] B. Ahmad, M.A. Ansari, P. Sen, R.H. Khan, Low versus high molecular weight poly(ethylene glycol)-induced states of stem bromelain at low pH: stabilization of molten globule and unfolded states, Biopolymers. 81 (2005) 350–359.

[15] H. Oliveira, V. Thiagarajan, M. Walmagh, S. Sillankorva, R. Lavigne, M.T. Neves-petersen, L.D. Kluskens, J. Azevedo, A Thermostable *Salmonella phage* Endolysin , Lys68, with broad bactericidal properties against gram-negative

pathogens in presence of weak acids, PLoS One. 9 (2014).

[16] C.O. Silva, S.B. Petersen, C.P. Reis, P. Rijo, J. Molpeceres, A.S. Fernandes, O. Gonçalves, A.C. Gomes, I. Correia, H. Vorum, M.T. Neves-petersen, EGF Functionalized polymer-coated gold nanoparticles promote EGF photostability and EGFR internalization for photothermal therapy, PLoS One. (2016) 1–29.

[17] C.O. Silva, S.B. Petersen, C.P. Reis, P. Rijo, J. Molpeceres, H. Vorum, M.T. Neves-petersen, Lysozyme photochemistry as a function of temperature. the protective effect of nanoparticles on lysozyme photostability, PLoS One. 10 (2015) 1–29.

[18] A.S.L. Carvalho, B.S. Ferreira, M.T. Neves-petersen, S.B. Petersen, M.R. Aires-barros, Heme and pH-dependent stability of an anionic horseradish peroxidase, Arch. Biochem. Biophys. 415 (2003) 257–267.

[19] C.L. Ginther, Sporulation and the- Production of Serine Protease and Cephamycin C by *Streptomyces lactamdurans*, Antimicrob. AGENTS Chemother. 15 (1979) 522–526.

[20] M.M. Bradford, A Rapid and Sensitive Method for the Quantitation Microgram Quantities of Protein Utilizing the Principle of Protein-Dye Binding, Anal. Biochem. 72 (1976) 248–254.

[21] Y. Fukunaga, Y. Katsuragi, T. Izumi, F. Sakiyama, Fluorescence characteristics of kynurenine and N'-formylkynurenine. Their use as reporters of the environment of tryptophan 62 in hen egg-white lysozyme., J. Biochem. 92 (1982) 129–141.

[22] J.S. Jacob, D.P. Cistola, F.F. Hsu, S. Muzaffar, D.M. Mueller, S.L. Hazen, J.W. Heinecke, Human phagocytes employ the myeloperoxidase-hydrogen peroxide system to synthesize dityrosine, trityrosine, pulcherosine, and isodityrosine by a

tyrosyl radical-dependent pathway, J. Biol. Chem. 271 (1996) 19950–19956.

[23] D.A. Malencik, S.R. Anderson, Dityrosine as a product of oxidative stress and fluorescent probe, Amino Acids. 25 (2003) 233–247.

[24] H. Alipour, A. Raz, S. Zakeri, N. Dinparast Djadid, Therapeutic applications of collagenase (metalloproteases): A review, Asian Pac. J. Trop. Biomed. 6 (2016) 975–981.

[25] R.X. Zhang, J.S. Gong, C. Su, D.D. Zhang, H. Tian, W.F. Dou, H. Li, J.S. Shi, Z.H. Xu, Biochemical characterization of a novel surfactant-stable serine keratinase with no collagenase activity from *Brevibacillus parabrevis* CGMCC 10798, Int. J. Biol. Macromol. 93 (2016) 843–851.

[26] M. Melikoglu, C.S.K. Lin, C. Webb, Kinetic studies on the multi-enzyme solution produced via solid state fermentation of waste bread by *Aspergillus awamori*, Biochem. Eng. J. 80 (2013) 76–82.

[27] M. Correia, V. Thiagarajan, I. Coutinho, G.P. Gajula, B. Petersen, Steffen, M.T. Neves-petersen, Modulating the structure of EGFR with UV light: New possibilities in cancer therapy, PLoS One. 9 (2014) 1–15.

[28] G. Güler, M.M. Vorob'ev, V. Vogel, W. Mäntele, Proteolytically-induced changes of secondary structural protein conformation of bovine serum albumin monitored by Fourier transform infrared (FT-IR) and UV-circular dichroism spectrosc, Spectrochim. Acta Part AMolecular Biomol. Spectrosc. 161 (2016) 8–18.

[29] L.J. Smith, K.M. Fiebig, H. Schwalbe, C.M. Dobson, The concept of a random coil. Residual structure in peptides and denatured proteins., Fold. Des. 1 (1996) R95-106.

[30] D. Feng, Y. Xue, Z. Li, Y. Wang, W. Yang, C. Xue, Dielectric properties of

myofibrillar protein dispersions from Alaska Pollock (*Theragra chalcogramma*) as a function of concentration, temperature, and NaCl concentration, J. Food Eng. 166 (2015) 342–348.

[31] A. Oseev, M.P. Schmidt, S. Hirsch, A. Brose, B. Schmidt, Two-component dielectric dispersion impedance biosensor for in-line protein monitoring, Sensors Actuators, B Chem. 239 (2017) 1213–1220.

[32] Y.Y. Sham, I. Muegge, A. Warshel, The effect of protein relaxation on charge-charge interactions and dielectric constants of proteins, Biophys. J. 74 (1998) 1744–1753.

[33] M.T. Neves-petersen, S.B. Petersen, M. Correia, M.T. Neves-petersen, P.B. Jeppesen, S. Gregersen, UV-Light Exposure of Insulin : Pharmaceutical Implications upon Covalent Insulin Dityrosine Dimerization and Disulphide Bond Photolysis, PLoS One. 7 (2012).

[34] L. Wu, Y. Sheng, J. Xie, W. Wang, Photoexcitation of tryptophan groups induced reduction of disulfide bonds in hen egg white lysozyme, J. Mol. Struct. 882 (2008) 101–106.

[35] J.R. Lakowicz, Principles of Fluorescence Spectroscopy, 2nd ed., Kluwer Academic /Plenum Pnbllihers, New York, 1999.

[36] J.J. Prompers, C.W. Hilbers, H.A.M. Pepermans, Tryptophan mediated photoreduction of disulfide bond causes unusual fluorescence behaviour of *Fusarium solani pisi* cutinase, FEBS Lett. 456 (1999) 409–416.

[37] B.A. Kerwin, R.L. Remmele, Protect from Light: Photodegradation and Protein Biologics, J. Pharm. Sci. 96 (2007) 1468–1479.

[38] M.T. Neves-petersen, S. Klitgaard, T. Pascher, E. Skovsen, T. Polivka, Flash Photolysis of cutinase: identification and decay kinetics of transient intermediates

formed upon UV excitation of aromatic residues, Biophys. J. 97 (2009) 211–226.

[39] M. Correia, T. Snabe, V. Thiagarajan, S.B. Petersen, S.R.R. Campos, A.M. Baptista, Photonic activation of plasminogen induced by low dose UVB, PLoS One. 10 (2017) 1–18.

[40] R. Amado, R. Aeschbach, H. Neukom, Dityrosine: In vitro production and characterization, Methods Enzymol. 107 (1984) 377 338.

[41] F. Sousa, B. Sarmento, M.T. Neves-petersen, Biophysical study of bevacizumab structure and bioactivity under thermal and pH-stresses, Eur. J. Pharm. Sci. 105 (2017) 127–136.

[42] O.S. da Silva, R.L. de Oliveira, J. de C. Silva, A. Converti, T.S. Porto, Thermodynamic investigation of an alkaline protease from *Aspergillus tamarii* URM4634: A comparative approach between crude extract and purified enzyme, Int. J. Biol. Macromol. 109 (2017) 1–6.

Figures captions

Fig. 1. pH dependence of the Far-UV CD spectra of the protease from *Aspergillus tamarii* URM4634 at 20°C (A), upon heating at 90°C (B) and upon cooling at 20°C (C). (D) Temperature dependence of the Far-UV CD spectra of the protease from *Aspergillus tamarii* URM4634 at pH 9.

Fig. 2. Fluorescence excitation spectrum (emission at 345nm) and fluorescence emission spectrum (excitation at 280nm) of a fresh sample of the protease from *Aspergillus tamarii* URM4634 at different pH values at 20°C (A) and respective normalized spectra of the fresh sample at 20°C (B), spectra at 20°C after cooling down the samples from 90°C (C) and respective normalized spectrum of the cooled sample at 20°C (D). pH dependence of the maximum fluorescence intensity of the protease before heating and after cooling (E) and pH dependence of the wavelengths corresponding to the maximum fluorescence emission intensity emitted by the protease before heating, upon heating and after cooling (F).

Fig. 3. Fluorescence excitation spectrum (emission at 345 nm) and fluorescence emission spectrum (excitation at 280 nm) of the protease from *Aspergillus tamarii* URM4634 at pH 6 before heating (20°C), upon heating (90°C) and after cooling (20°C).

Fig. 4. Fluorescence emission (spectra excitation at 295 nm) of the protease from *Aspergillus tamarii* URM4634 in different pH values of a fresh sample at 20°C (A), normalized spectrum of the fresh sample at 20°C (B), spectra at 20°C after cooling down the samples from 90°C (C), normalized spectrum of the sample upon cooling down at 20°C (D), pH dependence of the maximum fluorescence intensity of the protease before heating and after cooling (E) and pH dependence of the wavelengths corresponding to the maximum fluorescence emission intensity emitted by the protease before heating, upon heating and after cooling (F).

Fig. 5. Changes induced by temperature in the wavelength at which maximum protein fluorescence emission intensity is observed. During the heating run the protein has been excited at 280 or at 295 nm. Data retrieved from panels F in Figures 2 and 4.

$\Delta\lambda\lambda = \Delta\lambda_{(exc.\ 280nm)} - \Delta\lambda_{(exc.\ 295nm)}$.

Fig. 6. Monitoring the formation of photoproducts (NFK, Kyn and DT) before and after the heating run, from 20 to 90°C, during which the protein has been exposed to 280 nm light for 140 min. pH dependence of the fluorescence emission intensity (upon excitation at 320 nm) of a fresh sample of the protease from *Aspergillus tamarii* URM4634 at 20°C (A) and of the cooled sample at 20°C (B). pH dependence of the fluorescence excitation intensity (upon emission at 405 nm) of a fresh sample of the protease from *Aspergillus tamarii* URM4634 at 20°C (C) and of the cooled sample at 20°C (D).

Fig. 7. Monitoring the formation of photoproducts (NFK and Kyn) before and after the heating run, from 20 to 90°C, during which the protein has been exposed to 280 nm light for 140 min. pH dependence of the fluorescence emission intensity (upon excitation at 360 nm) of a fresh sample of the protease from *Aspergillus tamarii* URM4634 at 20°C (A) and of the cooled sample at 20°C (B). pH dependence of the fluorescence excitation intensity (upon emission at 435 nm) of a fresh sample of the protease from *Aspergillus tamarii* URM4634 at 20°C (C) and of the cooled sample at 20°C (D).

Fig. 8. (A) Normalized and fitted circular dichroism intensity data at 222 nm revealing the thermal unfolding of the protease from *Aspergillus tamarii* URM4634 as a function of pH. The heating run was carried out from 20 to 90°C at a heating rate of 1°C/min; (B) Thermal unfolding curves obtained by fluorescence spectroscopy. Fluorescence emission intensity was monitored at 345 nm, upon 280nm excitation as a function of pH; (C) Example of the fitting process (fluorescence spectroscopy data, pH 5) showing the first derivative of the fitted Boltzmann function (see insert) used to determine the melting temperature (60ºC) of the protein; (D) Thermal curves obtained with fluorescence spectroscopy upon cooling the protein sample from 90 to 20°C (fluorescence emission set at 345 nm, excitation at 280 nm).

Fig. 9. (A) Melting temperature (Tm) of the protease from *Aspergillus tamarii* URM4634 as a function of pH determined by CD and fluorescence spectroscopy (please see Table 2). (B) pH-stability and activity profiles of the protease from *Aspergillus tamarii* URM4634. See section 2.8 for experimental details.

Table 1: Fluorescence intensity and wavelength corresponding to the fluorescence maximum of *Aspergillus tamarii* URM4634 protease at different pH and temperature values.

	Emission spectrum (Exc. at 280 nm)			**Emission spectrum (Exc. at 295 nm)**			**Excitation spectrum (Em. at 345 nm)**		
pH	**Fresh Sample (20°C)**	**Upon heating (90°C)**	**Upon Cooling (20°C)**	**Fresh Sample (20°C)**	**Upon heating (90°C)**	**Upon cooling (20°C)**	**Fresh Sample (20°C)**	**Upon heating (90°C)**	**Upon cooling (20°C)**
	λ_{max}^{Em} (nm)	ΔF (%)	ΔF (%)	λ_{max}^{Em} (nm)	ΔF (%)	ΔF (%)	λ_{max}^{Exc} (nm)	ΔF (%)	ΔF (%)
5.0	340	-82.3	-26.2	340	-76.9	-31.0	286	-82.3	-26.2
6.0	338	-80.7	-22.1	335	-76.1	-34.3	286	-81.7	-28.4
7.2	343	-78.1	-11.8	341	-71.2	-27.4	285	-81.1	-27.4
8.0	342	-77.5	-20.6	341	-68.9	-29.8	285	-77.9	-26.2
9.0	345	-81.9	-15.3	346	-77.0	-19.7	286	-82.6	-20.4
10.0	348	-83.0	-7.5	350	-79.5	-10.8	286	-84.5	-13.8
11.0	352	-87.2	-13.8	353	-83.9	-12.9	287	-88.0	-13.5

$\boldsymbol{\lambda_{max}^{Em}}$ - Wavelength of the maximum fluorescence emission before heating (20°C); $\boldsymbol{\lambda_{max}^{Exc}}$ - Wavelength of the maximum fluorescence excitation before heating (20°C); **ΔF** - Fluorescence Intensity Decay (%). Intensity compared to value of a fresh sample at 20°C; **Fresh sample** – sample before heating; **Upon heating** – heating from 20 to 90°C; **Upon cooling** – after cooling from 90 to 20°C.

Table 2. Mathematical parameters recovered from the denaturation curves (monitored with FS and CD) acquired at different pH values and fitted by the Boltzmann decay model*. The recovered melting temperatures (X_0) are displayed in Figure 9A.

Fluorescence Parameters					
pHs	**A1**	**A2**	**X_0**	**dX**	**Adj. R^2**
pH 5	55647.1±61.6	15290.3±22.2	60.36±0.02	8.75±0.02	0.99
pH 6	71337.0±81.6	17901.0±30.9	59.22±0.02	10.05±0.02	0.99
pH 7.2	60646.5±100.9	19640.4±38.1	59.13±0.03	7.91±0.03	0.99
pH 8	74887.8±72.9	18812.6±24.4	53.23±0.02	9.30±0.02	0.99
pH 9	88472.7±197.9	15829.4±42.3	50.11± 0.06	12.73±0.03	0.99
pH 10	124817.9±96.4	14693.1±26.6	41.57±0.02	14.35±0.01	0.99
pH 11	140823.8±161.9	14539.9±27.0	37.99±0.03	13.88±0.02	0.99
Circular Dichroism Parameters					
pH	**A1**	**A2**	**X_0**	**dX**	**Adj. R^2**
pH 5	-2.58±0.00	-1.78±0.00	61.13±0.16	3.90±0.14	0.96
pH 6	-3.00±0.00	-1.33±0.00	67.80±0.09	4.61±0.09	0.99
pH 7.2	-2.46±0.00	-1.59±0.00	57.41±0.11	3.18±0.09	0.98
pH 8	-2.46±0.00	-1.60±0.00	54.89±0.11	3.46±0.10	0.97
pH 9	-3.36±0.00	-2.18±0.00	53.03±0.17	5.99±0.15	0.97
pH 10	-2.23±0.00	-1.50±0.00	48.71±0.17	4.34±0.15	0.96
pH 11	-1.83±0.00	-1.24±0.00	42.87±0.24	3.35±0.2	0.97

* $y = A2 + \frac{A1-A2}{1+ e^{(X-Xo)/dX}}$

A1 and A2 - Fit parameters corresponding to initial and final florescence intensity. **X_0** – Center, calculated melting point. **dX** – Time constant.

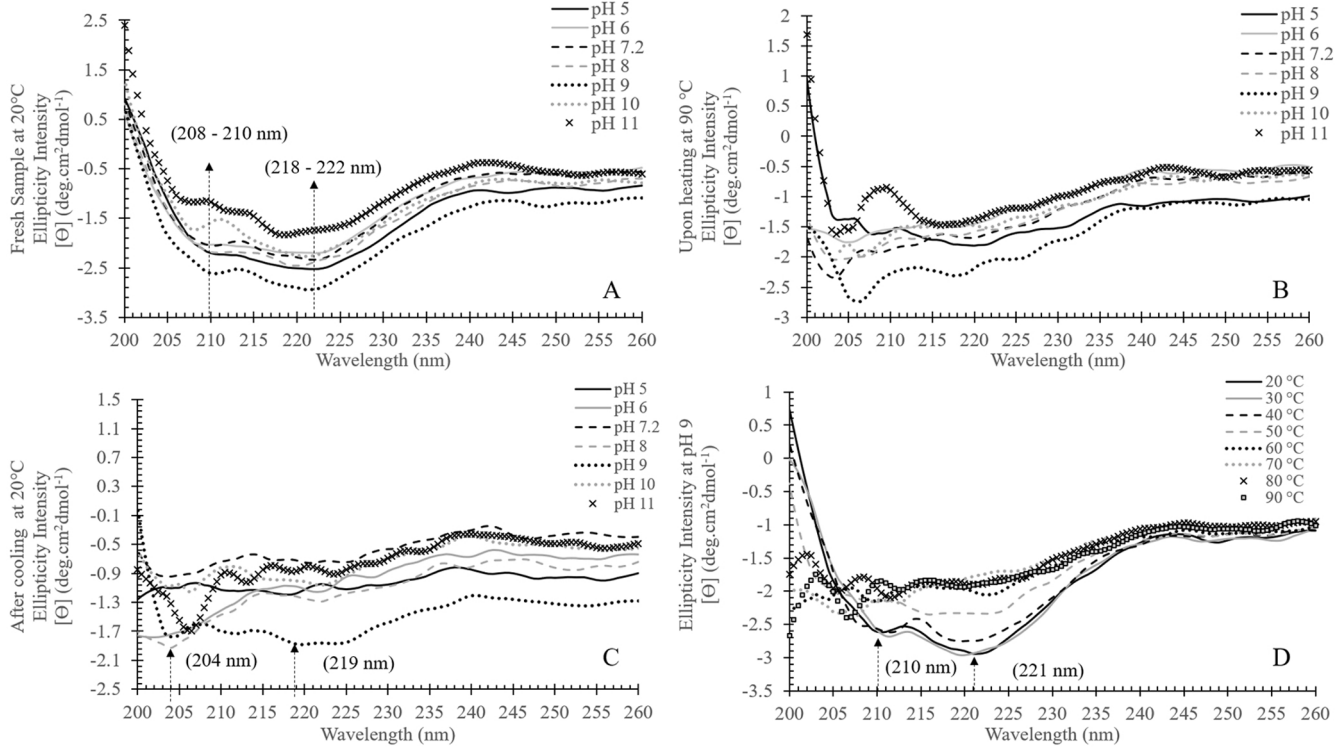
Fresh Sample at 20°C
Ellipticity Intensity
[Θ] (deg.cm²dmol⁻¹)
pH 5
pH 6
pH 7.2
pH 8
pH 9
pH 10
pH 11
(208 - 210 nm)
(218 - 222 nm)
A
Wavelength (nm)
Upon heating at 90 °C
Ellipticity Intensity
[Θ] (deg.cm²dmol⁻¹)
B
Wavelength (nm)
After cooling at 20°C
Ellipticity Intensity
[Θ] (deg.cm²dmol⁻¹)
(204 nm)
(219 nm)
C
Wavelength (nm)
Ellipticity Intensity at pH 9
[Θ] (deg.cm²dmol⁻¹)
20 °C
30 °C
40 °C
50 °C
60 °C
70 °C
80 °C
90 °C
(210 nm)
(221 nm)
D
Wavelength (nm)

Figure 1

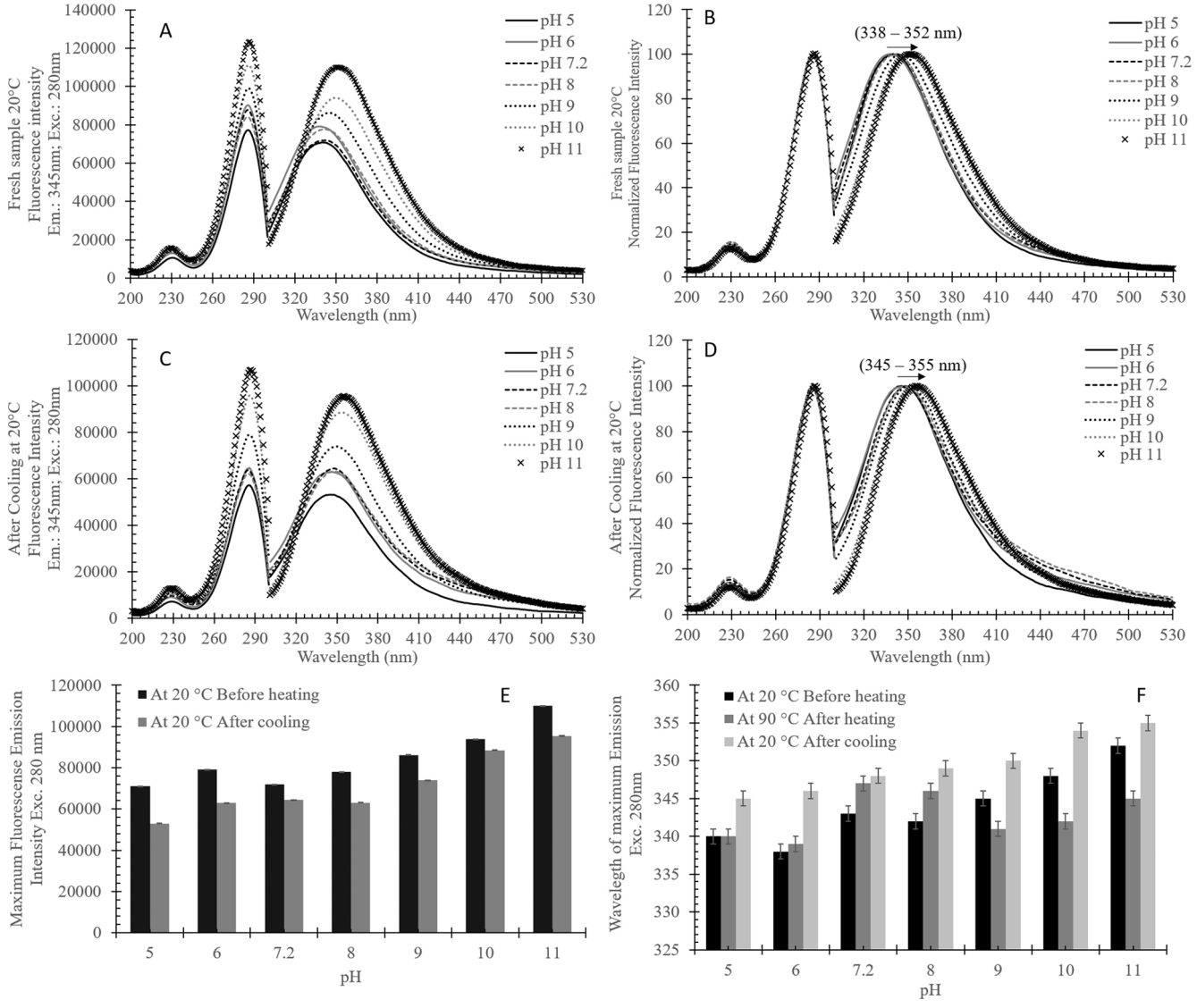
A
Fresh sample 20°C
Fluorescence intensity
Em.: 345nm; Exc.: 280nm
Wavelength (nm)
pH 5
pH 6
pH 7.2
pH 8
pH 9
pH 10
pH 11
B
(338 – 352 nm)
Fresh sample 20°C
Normalized Fluorescence Intensity
C
After Cooling at 20°C
Fluorescence Intensity
D
(345 – 355 nm)
After Cooling at 20°C
Normalized Fluorescence Intensity
E
At 20 °C Before heating
At 20 °C After cooling
Maximum Fluorescense Emission
Intensity Exc. 280 nm
pH
F
At 90 °C After heating
Wavelegth of maximum Emission
Exc. 280nm

Figure 2

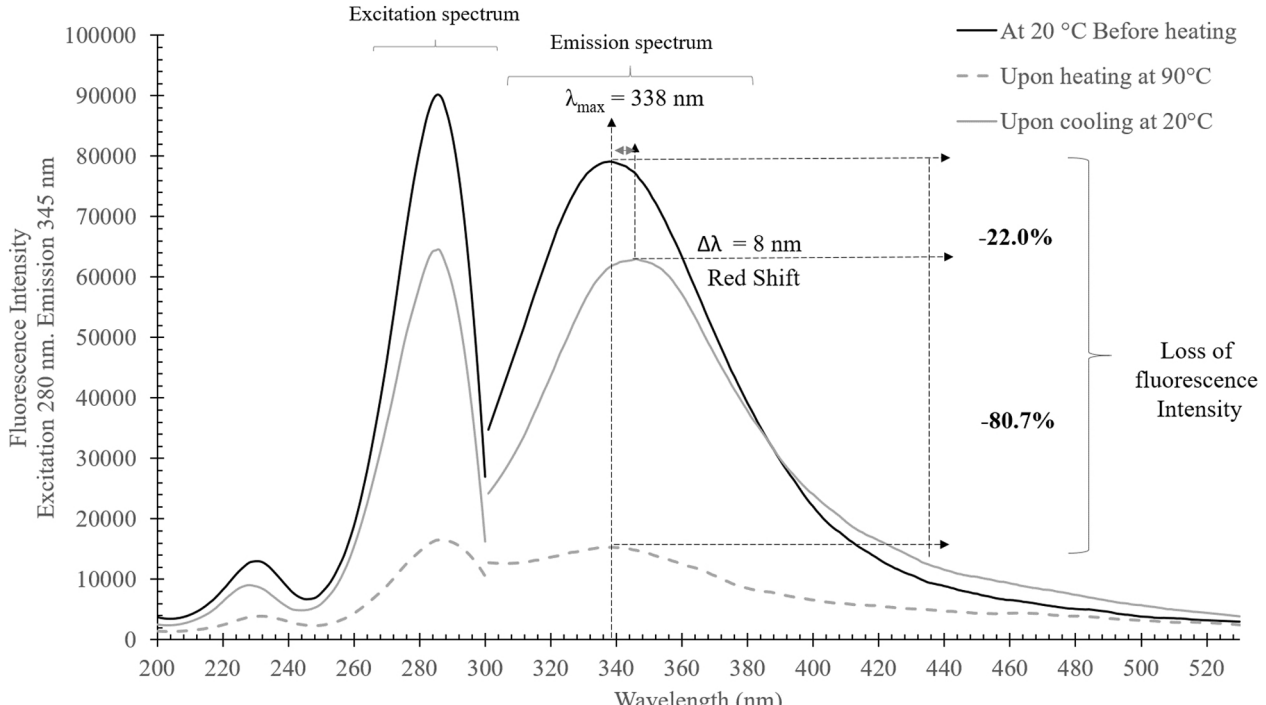
Excitation spectrum
Emission spectrum
λ_{max} = 338 nm
At 20 °C Before heating
Upon heating at 90°C
Upon cooling at 20°C
Δλ = 8 nm
Red Shift
-22.0%
-80.7%
Loss of fluorescence Intensity
Fluorescence Intensity
Excitation 280 nm. Emission 345 nm
Wavelength (nm)
100000
90000
80000
70000
60000
50000
40000
30000
20000
10000
0
200
220
240
260
280
300
320
340
360
380
400
420
440
460
480
500
520

Figure 3

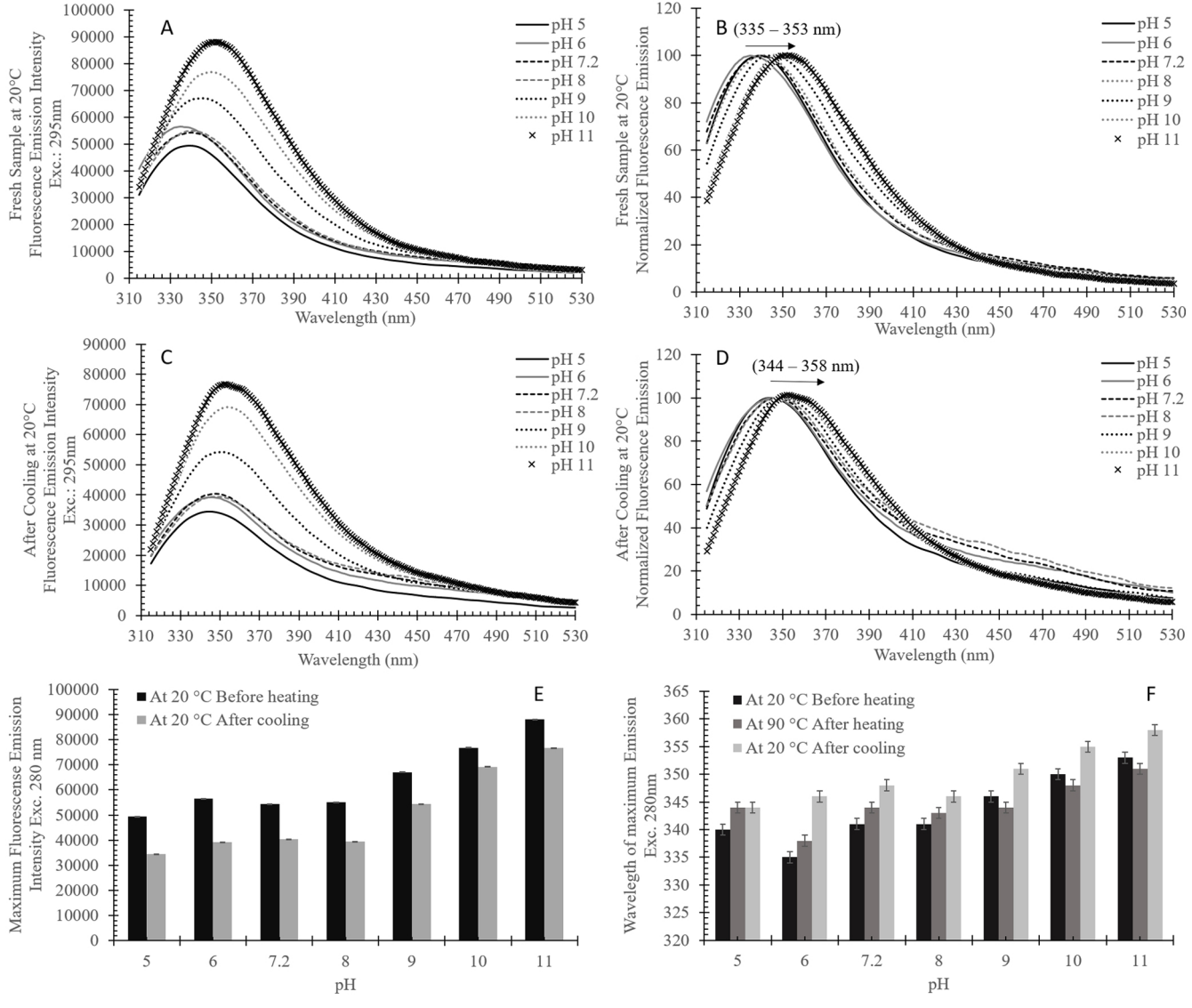
A
Fresh Sample at 20°C
Fluorescence Emission Intensity
Exc.: 295nm
Wavelength (nm)
pH 5
pH 6
pH 7.2
pH 8
pH 9
pH 10
pH 11
B (335 – 353 nm)
Fresh Sample at 20°C
Normalized Fluorescence Emission
C
After Cooling at 20°C
Fluorescence Emission Intensity
D (344 – 358 nm)
After Cooling at 20°C
Normalized Fluorescence Emission
E
At 20 °C Before heating
At 20 °C After cooling
Maximum Fluorescense Emission
Intensity Exc. 280 nm
pH
F
At 90 °C After heating
Wavelegth of maximum Emission
Exc. 280nm

Figure 4

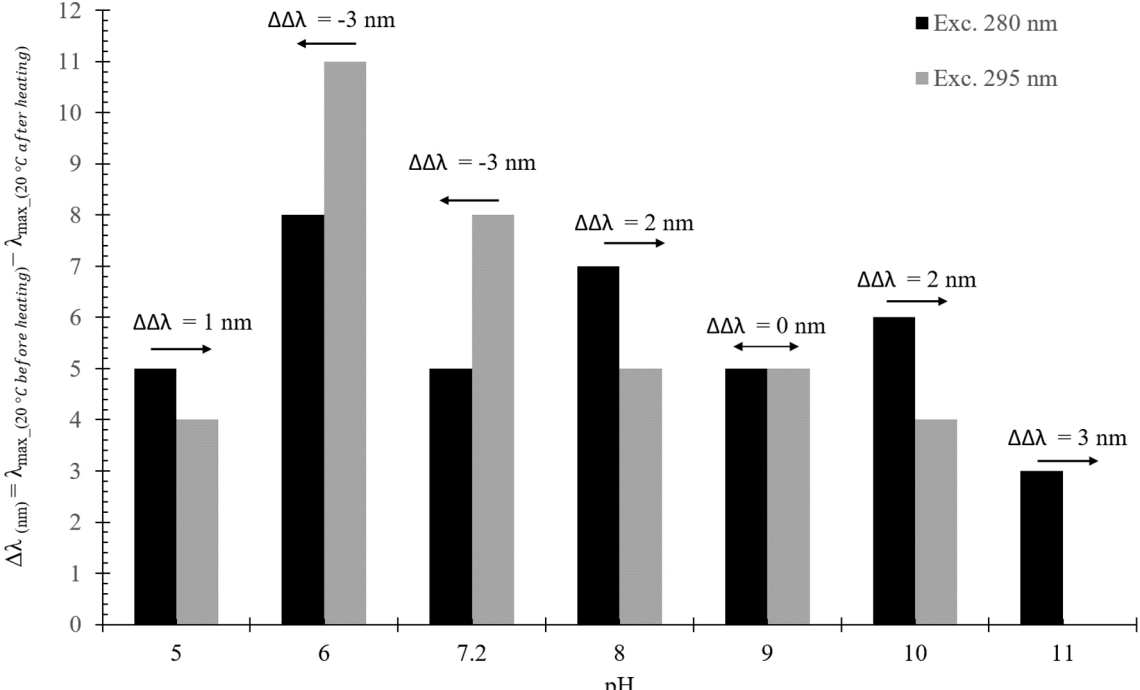
Exc. 280 nm
Exc. 295 nm
ΔΔλ = 1 nm
ΔΔλ = -3 nm
ΔΔλ = -3 nm
ΔΔλ = 2 nm
ΔΔλ = 0 nm
ΔΔλ = 2 nm
ΔΔλ = 3 nm
Δλ (nm) = λmax_(20 °C before heating) − λmax_(20 °C after heating)
pH
0
1
2
3
4
5
6
7
8
9
10
11
12
5
6
7.2
8
9
10
11

Figure 5

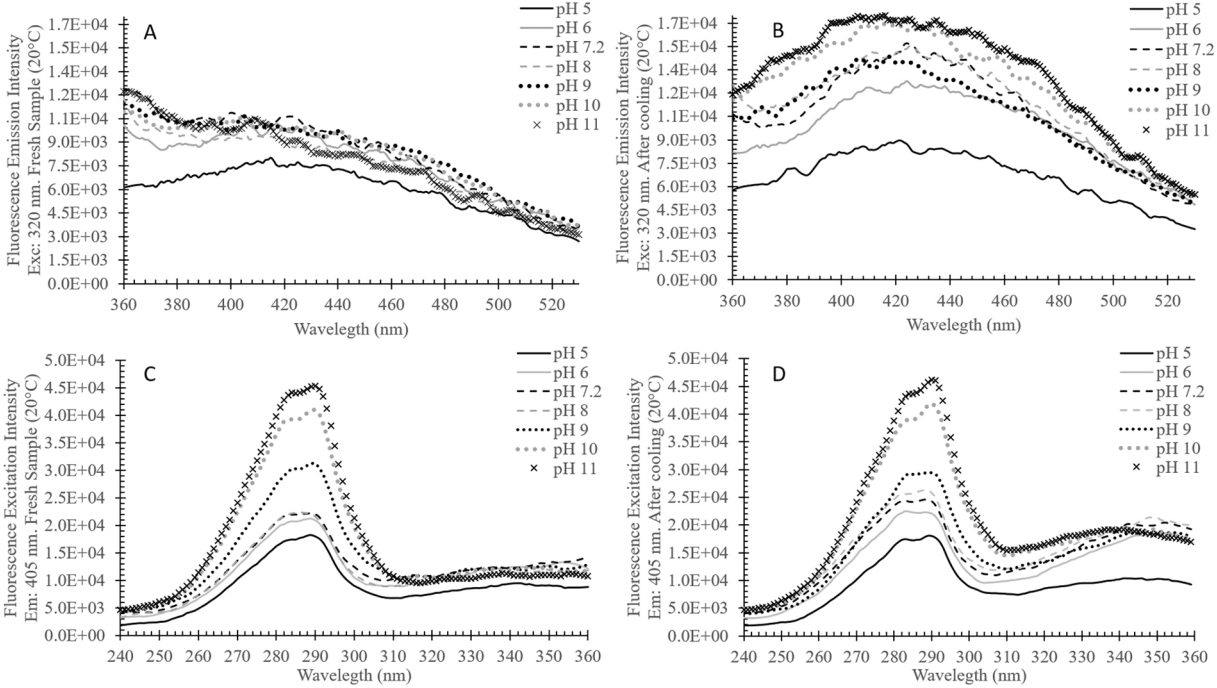
A
B
C
D
pH 5
pH 6
pH 7.2
pH 8
pH 9
pH 10
pH 11
Fluorescence Emission Intensity
Exc: 320 nm. Fresh Sample (20°C)
Fluorescence Emission Intensity
Exc: 320 nm. After cooling (20°C)
Fluorescence Excitation Intensity
Em: 405 nm. Fresh Sample (20°C)
Fluorescence Excitation Intensity
Em: 405 nm. After cooling (20°C)
Wavelegth (nm)

Figure 6

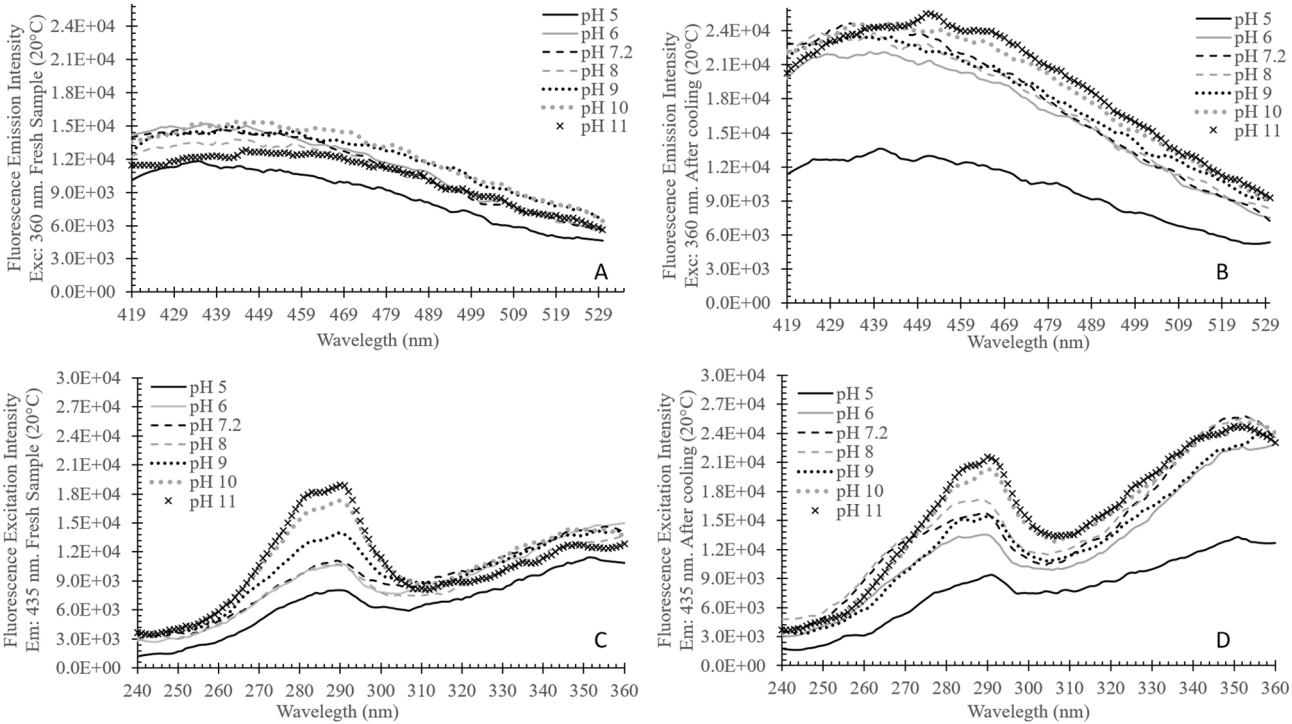
Fluorescence Emission Intensity
Exc: 360 nm. Fresh Sample (20°C)
Wavelegth (nm)
pH 5
pH 6
pH 7.2
pH 8
pH 9
pH 10
pH 11
A
Fluorescence Emission Intensity
Exc: 360 nm. After cooling (20°C)
Wavelegth (nm)
B
Fluorescence Excitation Intensity
Em: 435 nm. Fresh Sample (20°C)
Wavelegth (nm)
C
Fluorescence Excitation Intensity
Em: 435 nm. After cooling (20°C)
Wavelegth (nm)
D

Figure 7

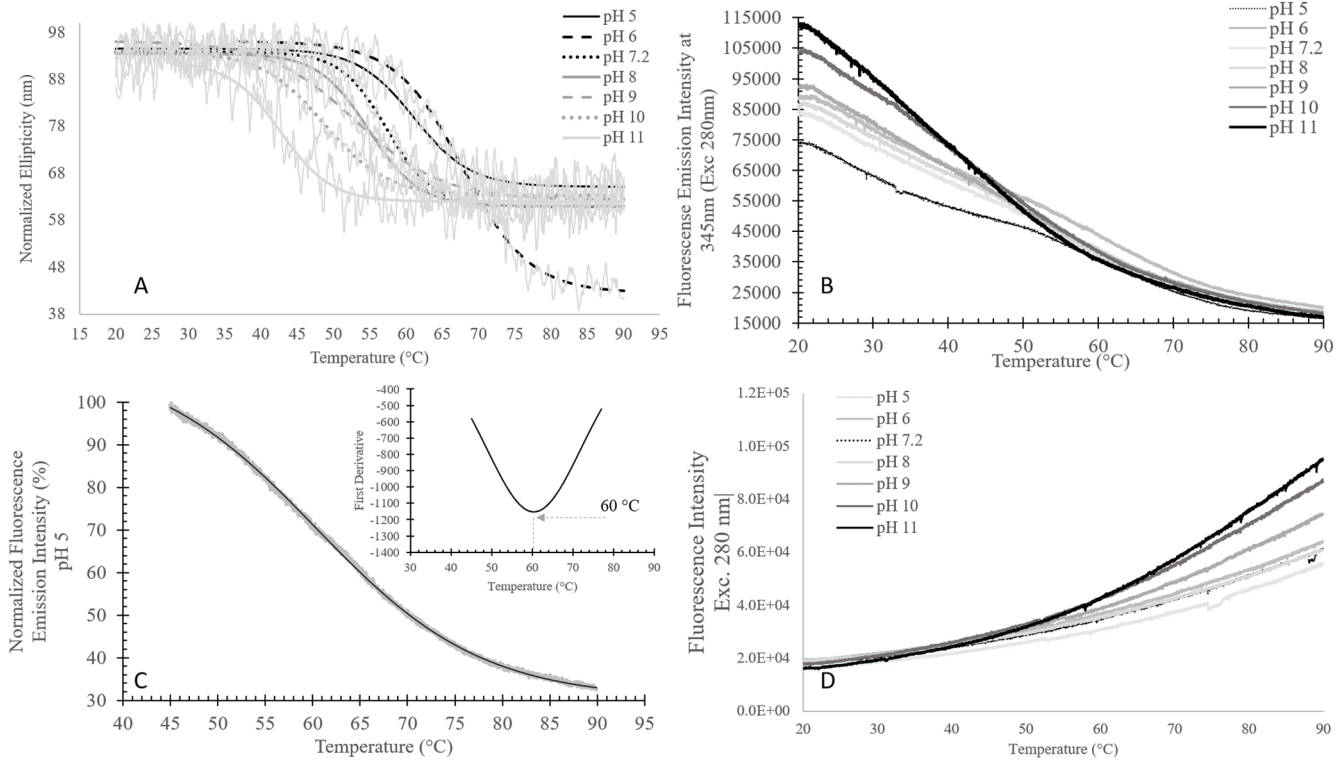
A
Normalized Ellipticity (nm)
Temperature (°C)
pH 5
pH 6
pH 7.2
pH 8
pH 9
pH 10
pH 11
B
Fluorescense Emission Intensity at 345nm (Exc 280nm)
Temperature (°C)
C
Normalized Fluorescence Emission Intensity (%) pH 5
First Derivative
60 °C
Temperature (°C)
D
Fluorescence Intensity Exc. 280 nm
Temperature (°C)

Figure 8

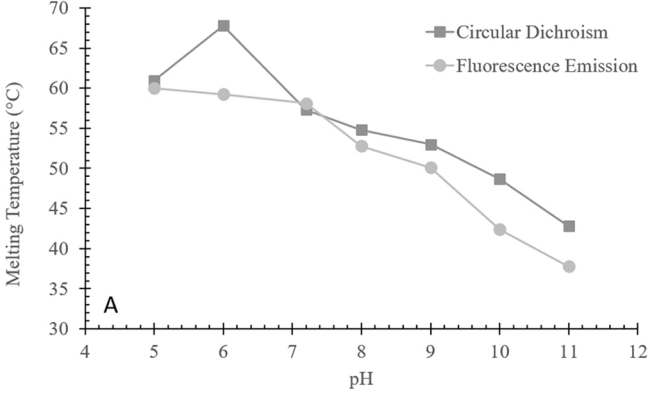
Melting Temperature (°C)
70
65
60
55
50
45
40
35
30
4
5
6
7
8
9
10
11
12
pH
Circular Dichroism
Fluorescence Emission
A

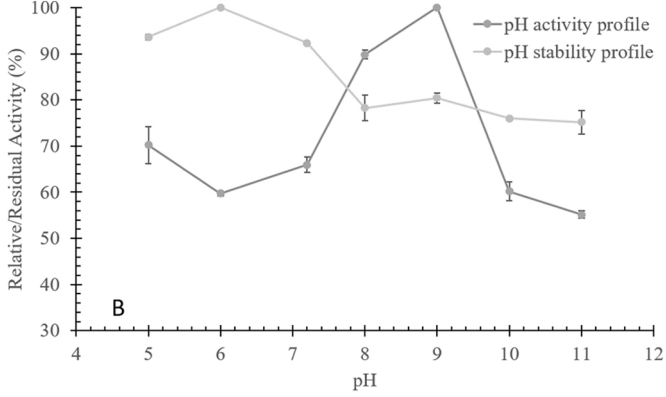
Relative/Residual Activity (%)
100
90
80
70
60
50
40
30
4
5
6
7
8
9
10
11
12
pH
pH activity profile
pH stability profile
B

Figure 9